# SYNTHESIS OF $TiO_2$-M (Cd, Co, Mn) AS A PHOTOCATALYST DEGRADATION OF METHYLENE BLUE DYE

**Candra Purnawan, Sayekti Wahyuningsih, Dwita Nur Aisyah**
*Sebelas Maret University (Indonesia)*

**Abstract.** $TiO_2$-M (M = Cd, Co, Mn) were synthesized by sol-gel method using titanium(IV) isopropoxide (TTIP) and cadmium sulfate octahydrate ($CdSO_4.8H_2O$), manganese(II) sulfate monohydrate ($MnSO_4.H_2O$), cobalt(II) sulfate heptahydrate ($CoSO_4.7H_2O$) as precursors. M-doped $TiO_2$ was performed with molar ratio 1:3; 1:2; 1:1; 2:1; 3:1 (mol Ti / mol M) and photocatalytic processes using visible light with irradiation time for 5, 10, 15, 20, 25 and 30 minutes. This study was carried out to determine the effect of different metal ions, the composition of Ti:M and the exposure time on the photocatalytic degradation of methylene blue dye. The results showed that different metal ions influenced crystal size and affected electronic properties (band gap). Crystal size of $TiO_2$ > $TiO_2$-Mn > $TiO_2$-Co > $TiO_2$-Cd and band gap of $TiO_2$ > $TiO_2$-Cd > $TiO_2$-Co > $TiO_2$-Mn. In addition, differences of Ti:M composition also influenced the photocatalytic activity. The longer of applied time exposure, the higher photocatalytic degradation of methylene blue was achieved. The optimum composition of Ti:M was obtained at Ti:M ratio by 3:1 with degradation values by 92.56% ($TiO_2$-Cd), 90.44% ($TiO_2$-Co), and 89.42% ($TiO_2$-Mn).

*Keywords*: methylene blue; metal doping; photocatalytic degradation; $TiO_2$-M; visible light

## Introduction

Indonesia is one of textile industrial based country producing wastewater. Most of wastewater generated from textile industry contain dyes which difficult to eliminate and to degrade. One of dyes often used in textile industry is methylene blue. Methylene blue, one of cationic dyes with chemical formula $C_{16}H_{18}ClN_3S$, is frequently employed in cotton, paper and hair dying process (Alzaydien, 2009). This aromatic hydrocarbon compound has strong adsorption and it was categorized as thiazine dyes. It also has toxic properties causing some effects in health, including skin irritation, cyanosis, and gastrointestinal track irritation (Hamdaoui & Chiha, 2007).

Nowadays, the researchers utilized $TiO_2$ semiconductor to degrade the dyes through photocatalytic, electrocatalyst, and photoelectrocatalyst degradation meth-

ods (Hamadanian et al., 2010; Purnawan et al., 2016; Wahyuningsih et al., 2013). The use of photocatalyst material, however, is limited since it only absorbs 5% ultraviolet light from sun with broad band gap: 3.0 – 3.2 eV (Ni et al., 2007). Thus, modification is required to improve optical property in visible light range.

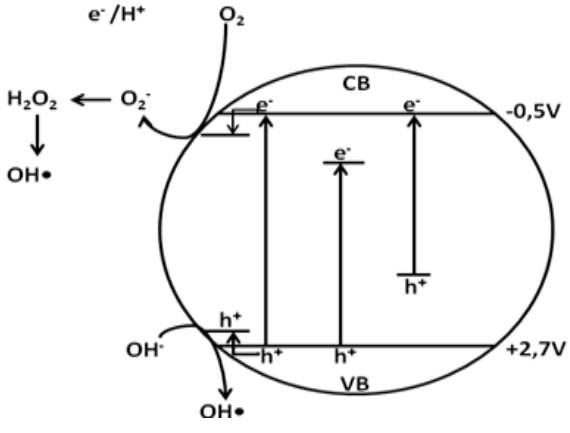


**Figure 1.** Photocatalytic mechanism of $TiO_2$ ($hv_1$ = origin $TiO_2$, $hv_2$ = metals ion doped $TiO_2$, $hv_3$ = non-metal doped $TiO_2$) (Zaleska, 2008)

Modification of $TiO_2$ can be performed by adding metals or doping metals like transition metals (Binas et al., 2012; Chen et al., 2005; Deng et al., 2011; Purnawan et al., 2016). The addition of metals into $TiO_2$ semiconductor with increasing concentration caused lowering band gap energy up to visible light absorption area (Ganesh et al., 2012; Tian et al., 2012).

Dopant ion formed electron trapping which it minimizes recombination process between electron and hole. Not only it resulted new band gap, metal doping also accelerated photocatalytic activities (El-Bahy et al., 2009; Zaleska, 2008). Fig. 1 illustrated the effect of metals doping on electron excitation of $TiO_2$ photocatalyst.

The addition of metals into $TiO_2$ semiconductor will decrease the particle size of doped semiconductor compared to the origin one. Introducing Cd metal into $TiO_2$ affected in lowering band gap of $TiO_2$/CdS (Li et al., 2014) and enhanced its photocatalytic activities in visible light (Shi et al., 2012). The decreasing of $TiO_2$ band gab and enhancing of its photocatalytic activities in visible light was also reported by adding Co (Miao et al., 2014; Yang et al., 2007) and Mn metals (Binas et al., 2012; Deng et al., 2011; Papadimitriou et al., 2011; Wang et al., 2015). The dopant Mn decreased the band gap thus it can be adsorbed the visible light. However, it could defect the $TiO_2$ crystal and reduce the photocatalytic activities when Mn metal was added in high concentration (Deng et al., 2011).

The $TiO_2$ doped with Mn (0.1%, 1% and 5%) degraded the methylene blue up to 70% by irradiating in visible light for 30 minutes (Binas et al., 2012; Papadimitriou et al., 2011). Another researcher, Wang et al. (2015), obtained optimum result by doping 6% Mn to $TiO_2$. They also found that by increasing Mn concentration increased the rutile phase which reduce the $TiO_2$ photocatalytic sensitivity. However, the comparative study of three kind of metals, Co, Cd and Mn, doping $TiO_2$ is not yet studied. Thus, in this research successfully prepared the $TiO_2$ doped metals (Co, Cd and Mn) and evaluated their photocatalytic performance on methylene blue degradation.

## Experimental

*Materials and instrument*

All reagents employed in this research were commercially available from E-Merck except mentioned. They were titanium(IV) isopropoxide (TTIP), $CdSO_4.8H_2O$, $MnSO_4.1H_2O$, $CoSO_4.7H_2O$, acetic acid glacial, and ethanol. The methylene blue dye was commercially available from Surakarta, Indonesia. Aquades was purchased from Chemistry Laboratory of Universitas Sebelas Maret. The Instruments used in this study were XRD (*X-Ray Diffraction*, Bruker), SEM-EDX (*Scanning Electron Microscopy – Energy Dispersive X-ray*), FTIR (*Spektrofotometer Fourier Transform Infrared*, Shimadzu 6000) and *visible* lamp osram ultra vitalux (300W 230V AC).

*Synthesis of $TiO_2$-M (Cd, Mn, Co)*

Titanium (IV) isopropoxide solution was hydrolyzed in acetic acid glacial solution at 14 ºC with solution ration 1:10 v/v. The mixture was stirred continuously until the white and viscous solution achieved. Then, it was heated at 90 ºC to obtain white gel form. Afterward, each $CdSO_4$, $MnSO_4$ or $CoSO_4$ solutions was added drop wise into $TiO_2$ gel. The ratio of each metal sulfate toward $TiO_2$ gel was 1:3, 1:2, 1:1, 2:1 and 3:1 mol/mol. After it was cooled at room temperature, the gel was dried at 150 ºC for 24 h, then calcined at 400 ºC at 2 h.

*Photocatalytic degradation of methylene blue*

Photodegradation of methylene blue was conducted by adding 0.3 g $TiO_2$-M powder into 30 mL of 5 $mg.L^{-1}$ methylene blue solution. Under stirring condition, the mixture was irradiated with visible light in Black Box reactor. The visible light irradiation was carried out at 5, 10, 15, 20, 25 and 30 minutes. Afterward, the solution was separated using centrifugation at 6000 rpm for around 3 minutes. The solution absorbance was then analyzed using UV-Vis spectrophotometer.

## Results and discussion

*Characterization of crystal structure and size by XRD*

The XRD characterization of $TiO_2$-M was conducted to evaluate crystallinity of $TiO_2$-M powder by comparing the samples diffractogram with JCPDS standard. It

was carried out on the 3:1 ($TiO_2$:M) ratio of synthesized $TiO_2$-M at 2thetha 15–85°. Based on the XRD spectra of $TiO_2$-M (3:1) showed in Fig. 2 can be seen the primary characteristic peak of $TiO_2$ at 2θ 25.490°, 37.792° and 48.043°. This peak was confirmed as anatase phase corresponding to JCPDS number 78-2486. This anatase peak was also observed in $TiO_2$-Cd, $TiO_2$-Co and $TiO_2$-Mn diffractograms.

**Table 1.** The crystal size of $TiO_2$ and $TiO_2$-M

| Material | Crystal size (nm) |
|---|---|
| $TiO_2$-Cd | 6,907 |
| $TiO_2$-Co | 7,223 |
| $TiO_2$-Mn | 7,404 |
| $TiO_2$ | 15,622 |

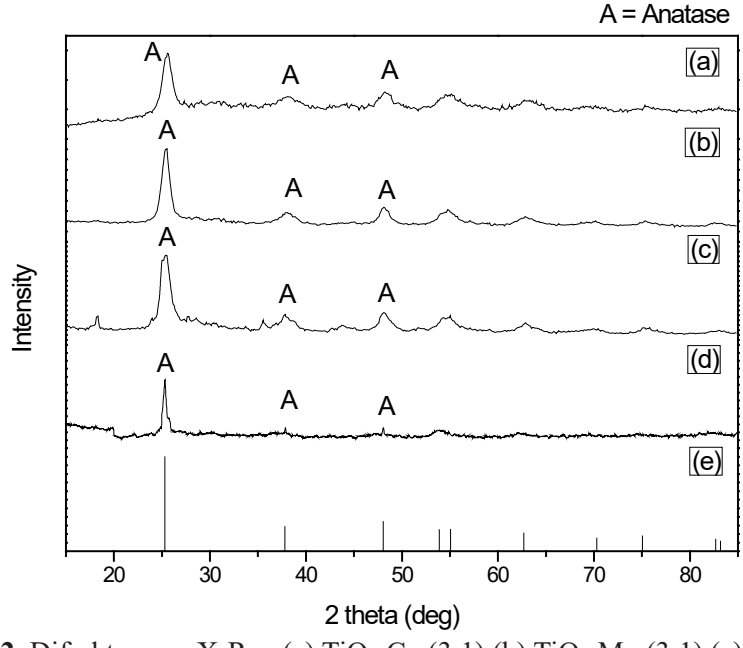


**Figure 2.** Difraktogram X-Ray (a) $TiO_2$-Co (3:1) (b) $TiO_2$-Mn (3:1) (c) $TiO_2$-Cd (3:1) (d) $TiO_2$ (e) JCPDS $TiO_2$ No 78-2486

The addition of metals into $TiO_2$ influenced the product crystal size. All of the $TiO_2$-M crystal size was lower than $TiO_2$. Comparing to another $TiO_2$-M, the $TiO_2$-Cd was the synthesized product having lowest crystal size, as shown in Table 1. This phenomena was also discovered by Deng et al. (2011), where after Mn metals was doped into $TiO_2$, it resulted 7 nm of $TiO_2$-Mn crystal size.

*Morphological study of $TiO_2$-M*

Morphological study of $TiO_2$-Cd, $TiO_2$-Mn and $TiO_2$-Co was conducted at each $TiO_2$:M ratio by 3:1. All of the $TiO_2$-M surface morphology was offered in Fig. 3. All of the measurement were captured at magnificent 5000x. The morphology of $TiO_2$-M was not significantly different observed in this research. This indicated that the addition of metals was not change the morphology of $TiO_2$-M. From the SEM image was calculated the particle size distribution using JImage application. The calculation result gave same values, where the particle size of $TiO_2$-M was distributed in range of 100-200 nm. Fig. 4 revealed the particle size distribution of each $TiO_2$-M.

The SEM-EDAX result showed that the doped metal concentration contained in $TiO_2$-M as presented in Table 2 were 8.62, 3.26 and 7.21% for Cd, Co and Mn, respectively. It was mean that the Cd was easily doped into $TiO_2$ than Co or even Mn. This was caused by the ionic radius of Cd was higher than Co and Mn, however its covalent radius of ionic hydrant was smaller than others, i.e. Cd (144±9 pm) < Co (150±7 pm) < Mn (161±8 pm). Due to it has small covalent radius of ionic hydrant, the Cd ion was readily to bind and to attach into $TiO_2$ semiconductor.

**Table 2.** Elemental analysis of $TiO_2$-M generated from SEM-EDAX

| Elements | Composition (%) | | |
|---|---|---|---|
| | $TiO_2$-Cd | $TiO_2$-Mn | $TiO_2$-Co |
| C | 5,76 | 4,59 | 6,13 |
| O | 29,50 | 38,14 | 33,53 |
| M (Cd, Mn or Co) | 8,62 | 3,26 | 7,21 |
| Ti | 53,54 | 51,85 | 51,83 |

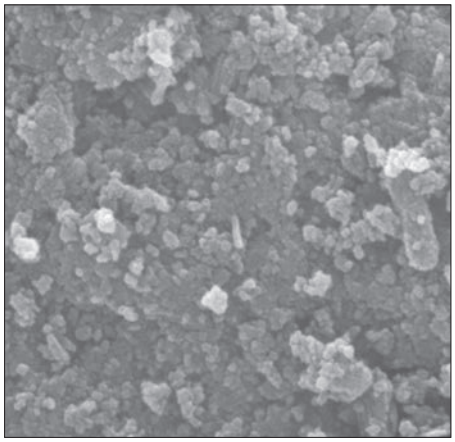

**(a)**

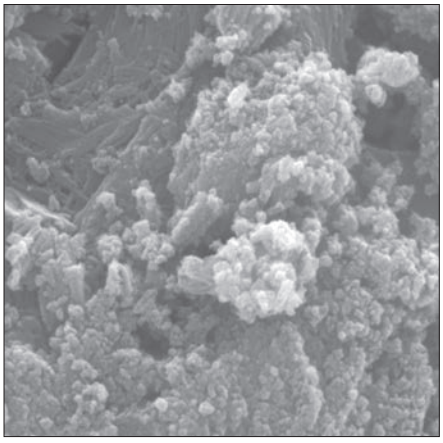

**(b)**

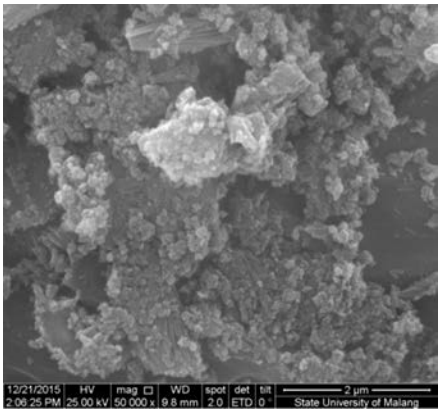


**(c)**

**Figure 3.** Morphology of (a) $TiO_2$-Cd, (b) $TiO_2$-Mn and (c) $TiO_2$-Co

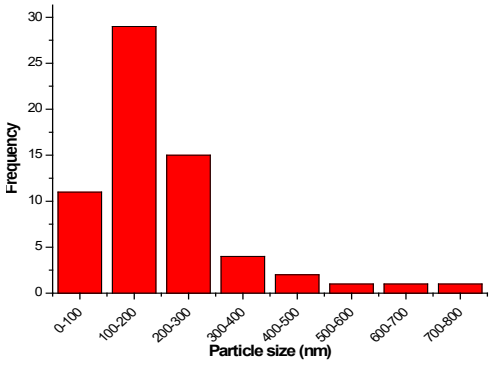


**(a)**

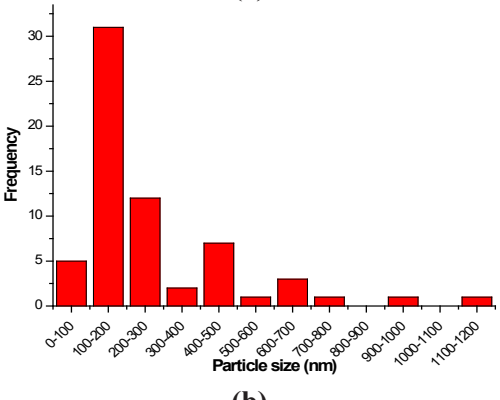


**(b)**

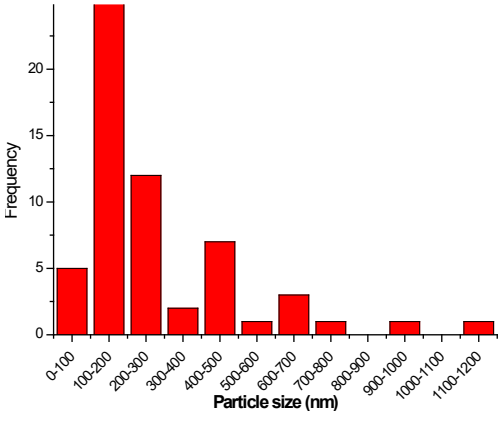


**(c)**

**Figure 4.** Particle size distribution of (a) $TiO_2$-Cd, (b) $TiO_2$-Mn and (c) $TiO_2$-Co

*Band gap energy*

The band gap energy was conducted via thin layer method. The $TiO_2$ and $TiO_2$-M samples was transformed to the transparency film at glass substrate then their absorbance were recorded using UV-Vis spectrophotometer. The band gap was calculated using Touc Plot method, a method to determine band gap using extrapolate from E (eV) versus $(Ahv)^2$ as shown in Fig. 5. Based on the Touch Plot graph can be evaluated band gap energy of each samples presented in Table 3.

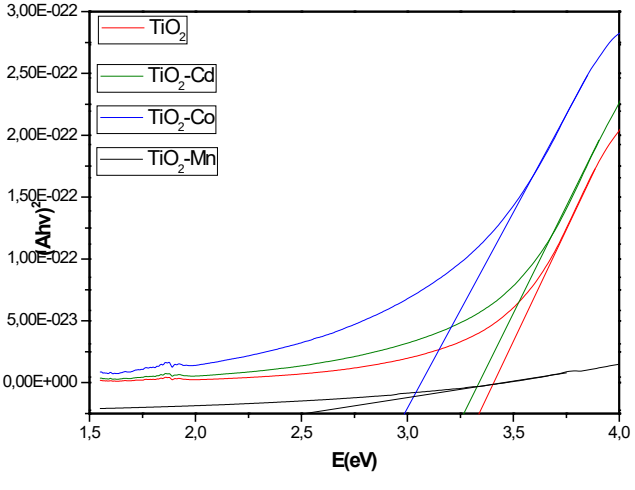


**Figure 5.** *Touc plot* graph of $TiO_2$ and $TiO_2$-M (3:1)

**Table 3.** The *band gap* and wave length values of $TiO_2$-M (3:1)

| Sampel | Band gap (eV) | λ (nm) |
|---|---|---|
| $TiO_2$ | 3,35 | 370,15 |
| $TiO_2$-Cd | 3,15 | 393,65 |
| $TiO_2$-Co | 3,00 | 413,33 |
| $TiO_2$-Mn | 2,5 | 496,00 |

The addition of metals into $TiO_2$ triggered the lowering band gap energy as presented in Table 3, the Eg of $TiO_2$> $TiO_2$-Cd > $TiO_2$-Co > $TiO_2$-Mn. The band gap energy of $TiO_2$-Mn was lowest to others $TiO_2$-M. This initiated a fast recombination of electron-hole which will inhibit oxidation reaction of methylene blue dye.

*FTIR analysis of $TiO_2$M*

Analysis of $TiO_2$-Cd using FTIR was performed to identify a bonding between Ti-O and Cd as result of Cd addition to $TiO_2$. In Fig. 6, the synthesized $TiO_2$ spectra has absorbance bands around 3405.47 $cm^{-1}$, 1627.99 $cm^{-1}$ as well as strong and broad band at 576.74 – 421.46 $cm^{-1}$ which they are characteristic band of $TiO_2$. The wave number at 3405.47 $cm^{-1}$ indicated the O-H stretching vibration of water entrapping in $TiO_2$ structure (Kuvarega et al., 2011). Another characteristic peak of water was also observed around 1625 – 1650 $cm^{-1}$ corresponding to the O-H bending vibration. The vibration of O-Ti-O was also discovered in the IR spectra at around 609.5 – 420.5 $cm^{-1}$ (Wahyuningsih et al., 2013).

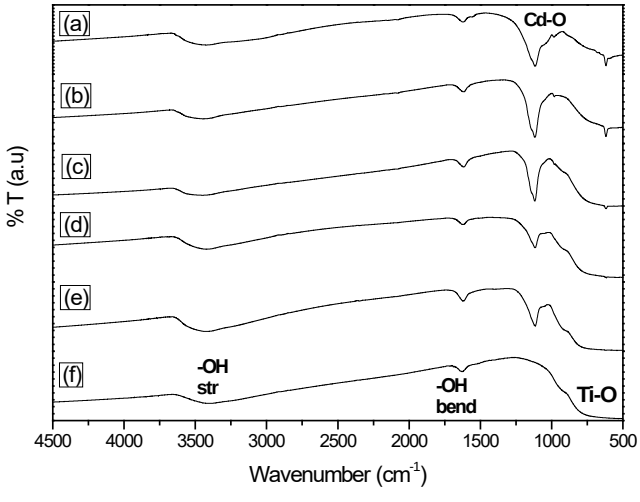


**Figure 6.** IR spectra of $TiO_2$-Cd, with ratio (a) 1:3 (b) 1:2 (c) 1:1 (d) 2:1 (e) 3:1, dan (f) $TiO_2$

The IR spectrum of $TiO_2$-Cd showed the broad absorbance band at around 3400 $cm^{-1}$ indicating the O-H stretching vibration (Kuvarega et al., 2011). The water characteristic band was also observed in $TiO_2$-Cd IR spectra appearing at 1600 $cm^{-1}$ (Li et al., 2011; Wu & Chen, 2004). A new absorbance band also appeared around 1115 – 1057 $cm^{-1}$ indicated the Ti-O-Cd stretching vibration. In addition, the absorbance band around 540 – 425 $cm^{-1}$ corresponding to Ti-O-Cd bending vibration. Both of this peaks were sharpen by decreasing of $TiO_2$: Cd ratio. This peaks related to the Ti-O-Cd bonding formation as result of Cd insertion in $TiO_2$.

The two peaks around 1100 $cm^{-1}$ and 980 $cm^{-1}$ were characteristic peak of Ti-O-Cd stretching vibration in accordance with what has been done by Ge (2012). Both of that peaks showed different intensity on each $TiO_2$: Cd composition ratio, the more concentration of Cd was added then the peak became sharpen. This also occurred at peak around 619.18 – 618.21 $cm^{-1}$ which corresponding to Cd stretching vibration.

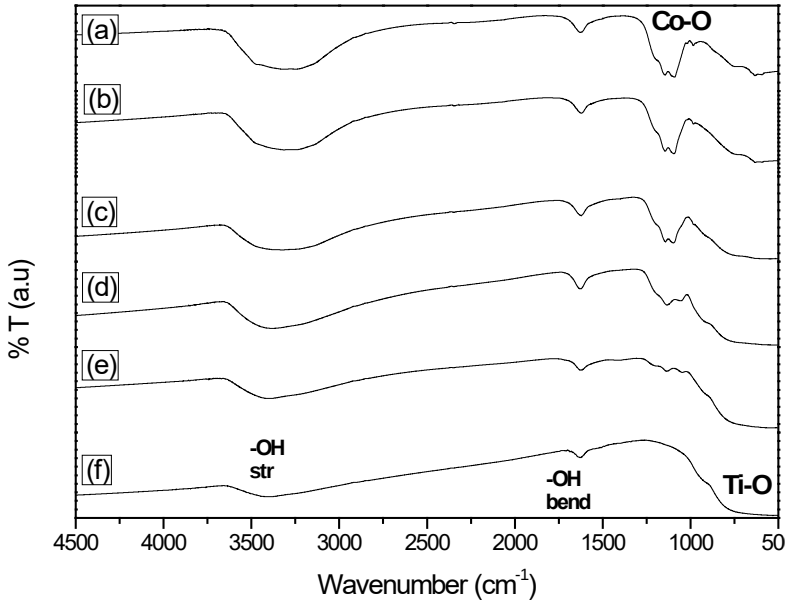


**Figure 7.** The $TiO_2$-Co IR spectrum at $TiO_2$ : Co ratio (a) 1:3 (b) 1:2 (c) 1:1 (d) 2:1 (e) 3:1, and (f) $TiO_2$

In $TiO_2$-Co IR spectra offered in Fig. 7 revealed a peak at 1627 $cm^{-1}$ corresponding to a bending vibration of H-O-H bonding. Peaks around 600 – 400 $cm^{-1}$ was an absorbance band of Ti-O-Ti. It was also exposed a weak and broad band around 2840 $cm^{-1}$ becoming strong peak by adding more Co, indicate the OH absorbance band of $H_2O$ bonded to Co-O. Absorbance band around 1000 – 1250 $cm^{-1}$ was a

characteristic peak of Co evidenced by increasing of its intensity with addition more concentration of Co while weaken by decreasing of Co composition (Ganesh et al., 2012).

A new absorbance band at 660 $cm^{-1}$ was found in $TiO_2$-Mn spectra presented in Fig. 8 indicating the β-$MnO_2$ vibration. Moreover, peaks at 620 $cm^{-1}$ and 530 $cm^{-1}$ was a characteristic vibration of O-Ti-O and Mn-O-Ti, respectively. Identification of $MnO_x$ was difficult to evaluate due to this peak over lapped with other peaks. This was also observed by other researchers (Kernazhitsky et al., 2010; Othman et al., 2007; Šurca et al, 2006). However, a peak around 1140–997 $cm^{-1}$ was predicted as Mn-O characteristic absorbance band since its intensity became sharpen at high ratio of Cd.

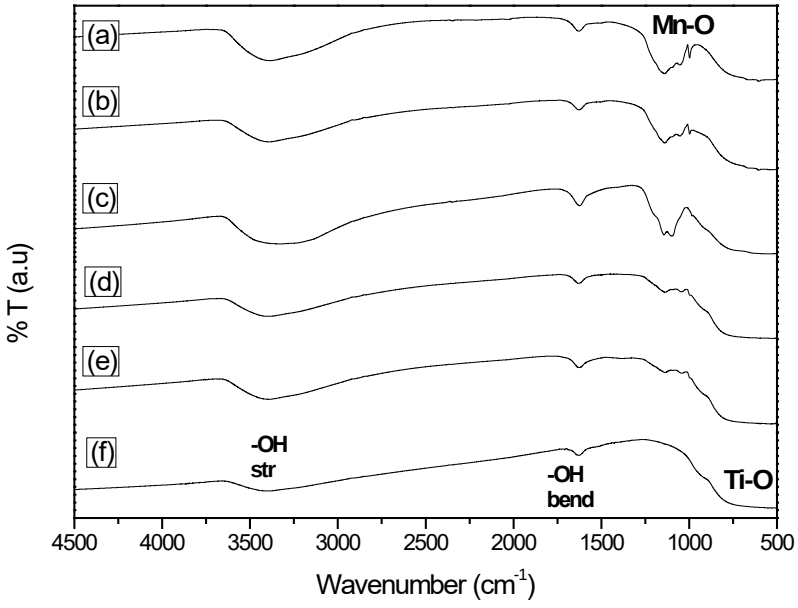


**Figure 8.** $TiO_2$-Mn IR spectrum with $TiO_2$ : Mn ratio (a) 1:3 (b) 1:2 (c) 1:1 (d) 2:1 (e) 3:1, and (f) $TiO_2$

*Photocatalytic degradation of methylene blue*

Qualitative analysis of methylene blue using UV-Vis spectrophotometer was conducted to determine its maximum wavelength ($\lambda_{maks}$). It was scanned in range of 800 nm – 350 nm with methylene blue concentration by 5 $mg.L^{-1}$. It was resulted that the maximum wavelength was obtained at 664 nm. This maximum wavelength was then used to identify the decreasing of methylene blue concentration in aqueous solution after photocatalytic degradation carried out.

This research focused to compare the photocatalytic activity of each $TiO_2$-M using visible light at same time and amount. After photocatalytic degradation, it was observed that the absorbance of methylene blue decreased. Photocatalytic degradation is a reaction process involved catalyst assisted with a photon. Fig. 9 showed the degradation result of each $TiO_2$-Cd composition. All of composition revealed that the longer of contact time, the degradation percentages enhanced. They resulted a degradation closing to 90% at 30 minutes. The role on photocatalytic degradation was obtained as follow $TiO_2$-Cd (3:1) > (2:1) > (1:3) > (1:2) > (1:1). The same pattern was also discovered for $TiO_2$-Co and $TiO_2$-Mn where the highest degradation percentages was achieved at $TiO_2$:M ratio 3:1 while the lowest was at 1:1. The percentage degradation data of $TiO_2$-Co and $TiO_2$-Mn were presented in Fig. 10 and Fig. 11, respectively.

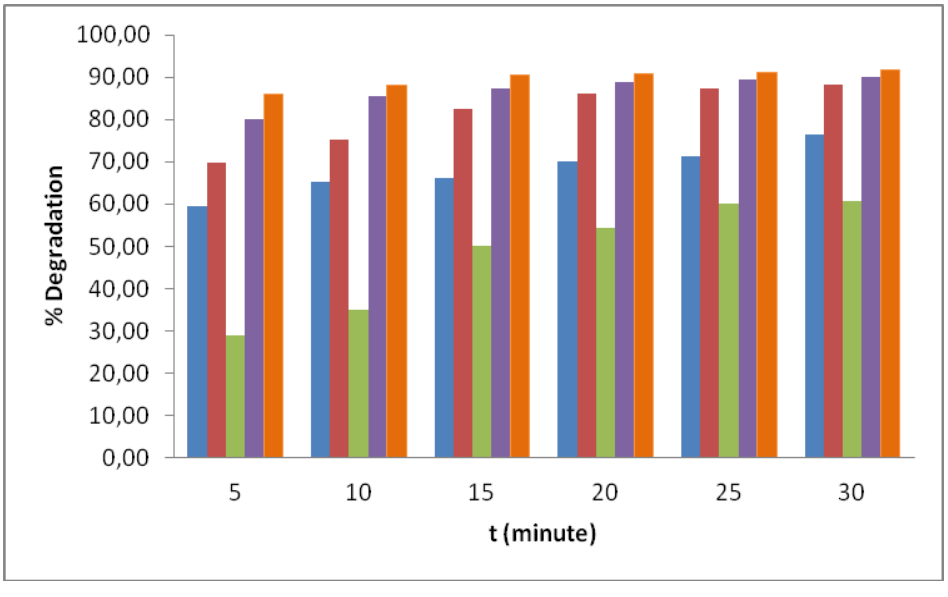


**Figure 9.** Methylene blue degradation percentages using $TiO_2$-Co at ratio $TiO_2$:Co = 1:3 (blue); 1:2 (red); 1:1 (green); 2:1 (violet) and 3:1 (orange)

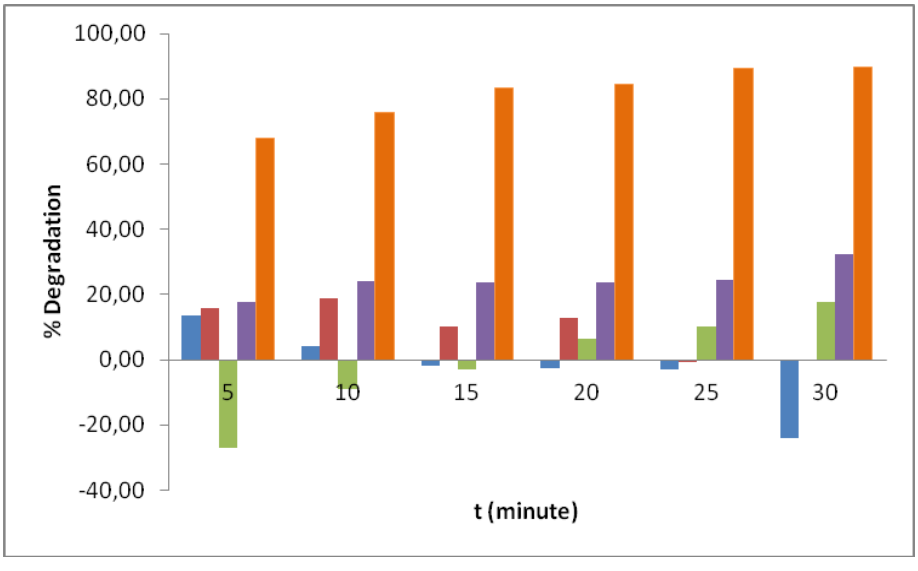


**Figure 10.** Methylene blue degradation percentages using $TiO_2$-Mn at ratio $TiO_2$:Mn = 1:3 (blue); 1:2 (red); 1:1 (green); 2:1 (violet) and 3:1 (orange)

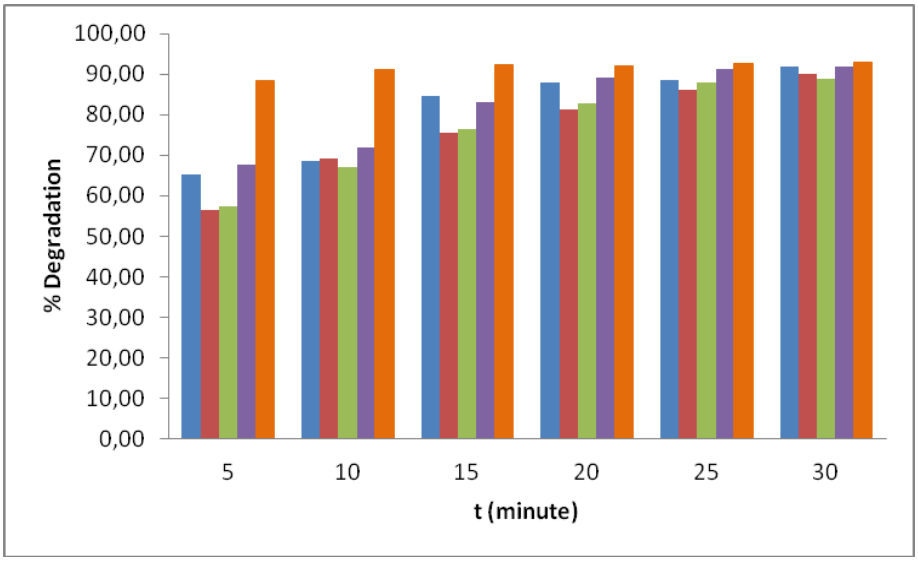


**Figure 11.** Methylene blue degradation percentages using $TiO_2$-Cd at ratio $TiO_2$:Cd = 1:3 (blue); 1:2 (red); 1:1 (green); 2:1 (violet) and 3:1 (orange)

The addition of high concentration of metals caused on decreasing of photocatalytic activity. High metal concentration has high number of defect structure and created more trapper. It triggered a charge carrier generated from energy induction result on $TiO_2$ photocatalyst can stuck more than one time thus it slow down the mobility and it could undergo a recombination before reaching photocatalyst surfaces. This phenomena initiating at high composition of dopant resulted low degradation percentage compared to a sample added by low composition of dopant.

Based on the experiment result can be revealed that the optimum composition of all $TiO_2$-M was obtained at ratio 3:1. In addition, $TiO_2$-Cd was the best formulation compared to others $TiO_2$-M with degradation percentages of 92.83% followed by $TiO_2$-Co and $TiO_2$-Mn which they had degradation percentages of 91.64% and 89.79%, respectively as seen in Fig. 12.

The Cd, Co and Mn have different ionic radius inducing the resulted $TiO_2$-M. The ionic radiation of $Cd^{2+}$ is larger than $Co^{2+}$ and $Mn^{2+}$. The metals, which have large ionic radius, were doped into $TiO_2$ reducing the steric hydrant and make them easily to interact with oxygen thus a bonding with $TiO_2$ semiconductor was effortlessly achieved. The Mn, however, has small ionic radius causing the entrance to $TiO_2$ difficult to accomplish due to it has high steric hydrant.

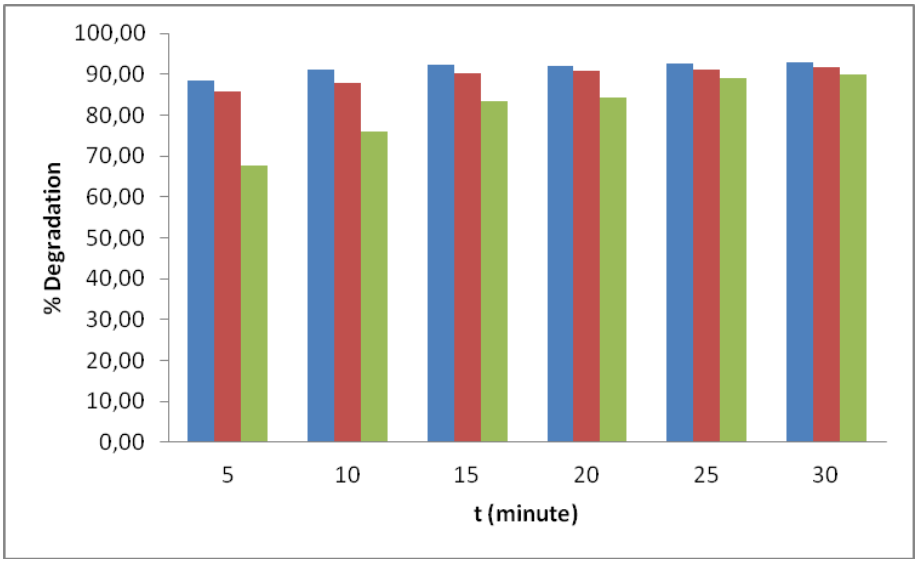


**Figure 12.** Methylene blue photocatalytic degradation percentages by $TiO_2$-Cd (3:1, blue), $TiO_2$-Co (3:1, red), $TiO_2$-Mn (3:1, green)

The photocatalytic activity was also influenced by oxidation number where the oxidation number of Cd < Co < Mn. The more of oxidation number of metals affected the number of species also more diverse thus the formed catalyst became irregular. This generated that $TiO_2$-Mn has low degradation percentages than others. Moreover, the band gap energy of $TiO_2$-Cd > $TiO_2$-Co > $TiO_2$-Mn also influenced in the photocatalytic activity because of the broad band gab will slow down electron-hole recombination process. All of that metals have reduction potential, where Cd < Co < Mn. The lower of their reduction potential, the more easily they oxidized and more stable in excitation state thus the number of empty orbital as an electron trap increased and recombination process became longer.

Photocatalyst degradation process was determined by reaction rate constant values (k) to identify the reaction kinetic on methylene blue degradation following first, second and third order reaction using Eqs. (1-3), respectively. From the first, second and third order reaction graphs was pointed the linearity value ($R^2$). The $R^2$ value closing to 1 showed the occurring order reaction and degradation of methylene blue. The k and R value of $TiO_2$-M was presented in Table 4.

$$\ln C = -k.t + \ln Co \quad (1)$$

$$\frac{1}{C} = k.t + \frac{1}{Co} \quad (2)$$

$$\frac{1}{C^2} - \frac{1}{Co^2} = 2k.t \quad (3)$$

**Table 4.** The reaction rate constant (*k*) and R values of methylene blue photocatalyst degradation by $TiO_2$-M 3:1

| | Kinetic model | k (ppm.menit-1) | R2 |
|---|---|---|---|
| $TiO_2$-Cd (3:1) | First order | 0,0162 | 0,734 |
| | Second order | 0,0354 | 0,771 |
| | Third order | 0,0786 | 0,805 |
| $TiO_2$-Mn (3:1) | First order | 0,0469 | 0,963 |
| | Second order | 0,0542 | 0,967 |
| | Third order | 0,0682 | 0,930 |
| $TiO_2$-Co (3:1) | First order | 0,0089 | 0,972 |
| | Second order | 0,0152 | 0,975 |
| | Third order | 0,0261 | 0,975 |

**Conclusion**

Synthesis of $TiO_2$ and $TiO_2$-M (M = Cd, Co and Mn) have been successfully conducted through sol-gel method. The addition of metals influenced on not only

the $TiO_2$ crystal growth but also the material electronic properties (Eg $TiO_2$ = 3,35 eV; $TiO_2$-Cd = 3,15 eV; $TiO_2$-Co = 3 eV dan $TiO_2$-Mn = 2,5 eV). The more metals ion doped into $TiO_2$ semiconductor affected on decreasing of photocatalytic activity. It was revealed that the optimum composition of $TiO_2$-M was obtained at $TiO_2$:M ratio by 3:1. The $TiO_2$-Cd optimum photocatalytic degradation value was 92.56% followed by $TiO_2$-Co (90.44%) and $TiO_2$-Mn (89.42%) making it to be the best $TiO_2$-M composition compared to others.

## REFERENCES


Alzaydien, A.S. (2009). Adsorption of methylene blue from aqueous solution onto a low- cost natural Jordanian Tripoli. *Amer. J. Environ. Sci.*, *5*, 197 – 208.

Binas, V.D., Sambani, K., Maggos, T., Katsanaki, A. & Kiriakidis, G. (2012). Synthesis and photocatalytic activity of Mn-doped $TiO_2$ nanostructured powders under UV and visible light. *Appl. Catalysis B: Environmental*, *113 – 114*, 79 – 86.

Chen, X., Lou, Y., Dayal, S., Qiu, X., Krolicki, R., Burda, C. & Becker, J. (2005). Doped semiconductor nanomaterials. *J. Nanosci. & Nanotech.*, *5*, 1408 – 1420.

Deng, Q.R., Xia, X.H., Guo, M.L., Gao, Y. & Shao, G. (2011). Mn-doped $TiO_2$ nanopowders with remarkable visible light photocatalytic activity. *Materials Lett. 65*, 2051 – 2054.

El-Bahy, Z.M., Ismail, A.A. & Mohamed, R.M. (2009). Enhancement of titania by doping rare earth for photodegradation of organic dye (Direct Blue). *J. Hazardous Materials*, *166*, 138 – 143.

Ganesh, I., Gupta, A.K., Kumar, P.P., Chandra Sekhar, P.S., Radha, K., Padmanabham, G. & Sundararajan, G. (2012). Preparation and characterization of Co-doped $TiO_2$ materials for solar light induced current and photocatalytic applications. *Materials Chem. & Phys., 135*, 220 – 234.

Ge, L., Zuo, F., Liu, J., Ma, Q., Wang, C., Sun, D., Bartels, L. & Feng, P. (2012). Synthesis and efficient visible light photocatalytic hydrogen evolution of polymeric g-$C_3N_4$ coupled with CdS quantum dots. *J. Phys. Chem. C*, *116*, 13708 – 13714.

Hamadanian, M., Reisi-Vanani, A. & Majedi, A. (2010). Sol-gel peparation and characterization of Co / $TiO_2$ nanoparticles: application to the degradation of methyl orange. *J. Iranian Chem. Soc., 7*, S52 – S58.

Hamdaoui, O. & Chiha, M. (2007). Removal of methylene blue from aqueous solutions by wheat bran. *Acta Chim. Slov*, *54*, 407 – 418.

Kernazhitsky, L., Shymanovska, V., Gavrilko, T., Puchkovska, G., Naumov, V., Khalyavka, T., Kshnyakin, V., Chemyak, V. & Baran, J. (2010).

Optical and photocatalytic properties of titanium-manganese mixed oxides. *Materials Sci. & Eng. B, 175*, 48 – 55.

Kuvarega, A.T., Krause, R.W.M. & Mamba, B.B. (2011). Nitrogen/palladium-codoped $TiO_2$ for efficient visible light photocatalytic dye degradation. *J. Phys. Chem. C*, *115*, 22110 – 22120.

Li, H., Lei, Y., Huang, Y., Fang, Y., Xu, Y., Zhu, L. & Li, X. (2011). Photocatalytic reduction of carbon dioxide to methanol by $Cu_2O$/SiC nanocrystallite under visible light irradiation. *J. Natural Gas Chem.*, *20*, 145 – 150.

Li, X., Xia, T., Xu, C., Murowchick, J. & Chen, X. (2014). Synthesis and photoactivity of nanostructured CdS-TiO2 composite catalysts. *Catalysis Today*, *225*, 64 – 73.

Miao, Y., Zhai, Z., Jiang, L., Shi, Y., Yan, Z., Duan, D., Zhen, K. & Wang, J. (2014). Facile and new synthesis of cobalt doped mesoporous $TiO_2$ with high visible-light performance. *Powder Technology*, *266*, 365 – 371.

Ni, M., Leung, M.K.H., Leung, D.Y.C. & Sumathy, K.. (2007). A review and recent developments in photocatalytic water-splitting using $TiO_2$ for hydrogen production. *Renewable &Sustainable Energy Rev., 11*, 401 – 425.

Othman, I., Mohamed, R.M. & Ibrahem, F.M. (2007). Study of photocatalytic oxidation of indigo carmine dye on Mn-supported $TiO_2$. *J. Photochem. & Photobiology A: Chemistry*, *189*, 80 – 85.

Papadimitriou, V.C., Stefanopoulos, V.G., Romanias, M.N., Papagiannakopoulos, P., Sambani, K., Tudose, V. & Kiriakidis, G. (2011). Determination of photo-catalytic activity of un-doped and Mn-doped $TiO_2$ anatase powders on acetaldehyde under UV and visible light. *Thin Solid Films*, *520*, 1195 – 1201.

Purnawan, C., Wahyuningsih, S. & Kusuma, P.P. (2016). Photocatalytic and photoelectrocatalytic degradation of methyl orange using graphite / $PbTiO_3$ composite, *Indones. J. Chem. 16*, 347 – 352.

Shi, J.W., Yan, X., Cui, H. J., Zong, X., Fu, M. L., Chen, S. & Wang, L. (2012). Low-temperature synthesis of CdS/$TiO_2$ composite photocatalysts: influence of synthetic procedure on photocatalytic activity under visible light. *J. Mol. Catalysis A: Chemical*, *356*, 53 – 60.

Šurca Vuk, A., Ješe, R., Gaberščček, M., Orel, B. & Dražič, G. (2006). Structural and spectroelectrochemical (UV-vis and IR) studies of nanocrystalline sol-gel derived $TiO_2$ films. *Solar Energy Materials & Solar Cells*, *90*, 452 – 468.

Tian, J., Deng, H., Sun, L., Kong, H., Yang, P. & Chu, J. (2012). Effects of Co doping on structure and optical properties of $TiO_2$ thin films prepared by sol–gel method. *Thin Solid Films*, *520*, 5179 – 5183.

Wahyuningsih, S., Purnawan, C., Kartikasari, P.A. & Praistia, N. (2013). Visible light photoelectrocatalytic degradation of rhodamine B using a dye-sensitised $TiO_2$ electrode. *Chem. Papers*, *68*, 1248 – 1256.

Wang, L., Zhang, X., Zhang, P., Cao, Z. & Hu, J. (2015). Photoelectric conversion performances of Mn doped $TiO_2$ under >420nm visible light irradiation. *J. Saudi Chem. Soc.*, *19*, 595 – 601.

Wu, J.C.-S. & Chen, C.-H. (2004). A visible-light response vanadium-doped titania nanocatalyst by sol-gel method. *J. Photochem. & Photobiology A: Chemistry, 163*, 509 – 515.

Yang, X., Cao, C., Hohn, K., Erickson, L., Maghirang, R., Hamal, D. & Klabunde, K. (2007). Highly visible-light active C- and V-doped $TiO_2$ for degradation of acetaldehyde. *J. Catalysis*, *252*, 296 – 302.

Zaleska, A. (2008). Doped-$TiO_2$: a review. *Recent Patents on Engineering, 2,* 157 – 164.

✉ **Candra Purnawan (corresponding author)**
Analytical and Environmental Chemistry Research Group
Chemistry Department
Sebelas Maret University
Surakarta, Central Java
57126 Indonesia
E-mail: candra_pr@staff.uns.ac.id